CSIRO PUBLISHING

RESEARCH PAPER
https://doi.org/10.1071/WF21005

International Journal of WILDLAND FIRE

International Association of Wildland Fire

Event-based quickflow simulation with OpenLISEM in a burned Mediterranean forest catchment

D. C. S. Vieira[A,B,*], M. Basso[B], J. P. Nunes[C,D], J. J. Keizer[B] and J. E. M. Baartman[C]

For full list of author affiliations and declarations see end of paper

***Correspondence to:**
D. C. S. Vieira
European Commission, Joint Research Centre (JRC), Ispra, Italy
Email: diana.simoes-vieira@ec.europa.eu

ABSTRACT

Recently burnt areas typically reveal strong to extreme hydrological responses, as a consequence of loss of protective soil cover and heating-induced changes in topsoil properties. Soil water repellency (SWR) has frequently been referred to as one of the explanatory variables for fire-enhanced surface runoff generation but this has been poorly demonstrated, especially at the catchment scale. This study employs a process-based modelling approach to better understand the relevance of SWR in the hydrological response of a small, entirely burnt catchment in central Portugal, in particular by comparing hydrological events under contrasting initial conditions of dry vs wet soils. The OpenLISEM model was applied to a selection of 16 major rainfall runoff events that occurred during the first 2 post-fire years. The automatic calibration procedure resulted in good model performance, but it worsened for validation events. Furthermore, uncertainty analysis revealed an elevated sensitivity of OpenLISEM to event-specific conditions, especially for predicting the events' total and peak flows. Also, predicted spatial patterns in runoff poorly agreed with the runoff observed in microplots. Model performance improved when events were separated by dry and wet initial moisture conditions, particularly for wet conditions, suggesting the role of variables other than initial soil moisture.

Keywords: autocalibration, catchment scale, eucalypt, event-based modelling, maritime pine, post-fire, rainfall-runoff modelling, soil moisture content, soil water repellency, surface runoff.

Received: 9 January 2021
Accepted: 10 May 2022
Published: 31 May 2022

Cite this:
Vieira DCS *et al.* (2022)
International Journal of Wildland Fire
doi:10.1071/WF21005

Introduction

During the last decades, wildfire occurrence has increased in the Iberian Peninsula, and the burnt area has, on average, exceeded 100 000 ha every year (San-Miguel-Ayanz *et al.* 2013). Wildfire frequency is expected to further increase in the future, owing to changes in climate and socio-economic drivers (Turco *et al.* 2014, 2016; Viedma *et al.* 2015; Calheiros *et al.* 2021).

The direct impacts of wildfires typically include the consumption of the vegetation and litter layer as well as heating-induced changes in topsoil properties (Shakesby and Doerr 2006; Moody *et al.* 2013; Ebel 2020). Thereby, wildfires decrease interception and increase both effective rainfall and rainfall erosivity (Cerdá and Doerr 2005; Stoof *et al.* 2012). Among the topsoil properties affected by fire, soil water repellency (SWR) has received much research attention because of its expected role in post-fire runoff generation (Doerr *et al.* 1996; DeBano 2000; Ferreira *et al.* 2000). SWR expresses the resistance of soils against wetting for periods ranging from seconds to weeks (DeBano 2000; Malvar *et al.* 2016; Mao *et al.* 2019). SWR is a highly dynamic property, varying between dry and wet seasons in both unburnt and burnt soils (Doerr *et al.* 2000; Santos *et al.* 2016; Martins *et al.* 2020). SWR severity has often been related to soil moisture content (SMC) but the fairly few high-resolution time series that exist to date have revealed complex relationships in burnt areas (Keizer *et al.* 2008; Malvar *et al.* 2016; Robichaud *et al.* 2016). This complexity has been explained by the existence of a so-called transition zone in SMC where soils can be both repellent and wettable (Crockford *et al.* 1991; Dekker *et al.* 2001). Because of SWR's dynamic nature, and the lack of non-destructive field

measurement methods, its contribution to post-fire runoff generation has been hard to quantify (Shakesby and Doerr 2006; Shakesby 2011).

The role of SWR in post-fire runoff generation has also been poorly explored using rainfall runoff models (Lopes *et al.* 2021). Post-fire hydrological modelling has focused on coarse temporal resolutions, with the bulk of the studies using a daily time-step (Dun *et al.* 2009; Seibert *et al.* 2010; Mahat *et al.* 2015; Moussoulis *et al.* 2015), and very few studies using a (sub-)hourly resolution (Canfield *et al.* 2005; Seibert *et al.* 2010; Van Eck *et al.* 2016; Rengers *et al.* 2016; Wu *et al.* 2021*a*, 2021*b*). Overall, efforts to assess model suitability for post-fire conditions have suffered from the lack of field data, as only a limited number of experimental catchments have been instrumented and monitored during the full window of disturbance period (Shakesby 2011; Moody *et al.* 2013). To date, only a handful of post-fire hydrological modelling studies have explicitly included the role of SWR. Liu *et al.* (2021) correlated temporal increases in saturated hydraulic conductivity with decreases in SWR due to the wet pre-event conditions. Vieira *et al.* (2014) simulated the role of SWR in the seasonal runoff response by reducing the effective infiltration depth in the Morgan–Morgan–Finney model with increasing SWR severity. Nunes *et al.* (2016) used the Thornthwaite–Mather model to simulate the role of SWR in post-fire infiltration through changes in daily soil moisture content, decreasing field capacity with increasing SWR severity. McGuire *et al.* (2018) assessed the use of spatial saturated hydraulic conductivity at catchment scale to simulate post-wildfire hydrological response and debris flow initiation under repellent conditions, finding the influence of sorptivity on infiltration rates to be negligible. Van Eck *et al.* (2016) is the only study at catchment scale that employed a process-based model to explore how variation in SWR affected the runoff response.

The present study is a follow-up of Van Eck *et al.* (2016) to improve the understanding of the hydrological response of recently burnt catchments and, in particular, the role therein of SWR, through the application of a process-based model (OpenLISEM). The role of SWR is explored by calibrating infiltration capacity for events with dry and repellent as well as wet and non-repellent antecedent conditions. To this end, an experimental catchment was selected that was small and entirely burnt, where SMC and SWR had been measured (Vieira *et al.* 2016, 2018), and for which the model input data requirements of OpenLISEM were met (see Van Eck *et al.* 2016).

The specific objectives were to: (i) quantify how well OpenLISEM could simulate the hydrological response at catchment scale for events with contrasting initial conditions of SMC and SWR; (ii) optimise OpenLISEM performance through a generalised calibration approach, adjusting maximum infiltration capacity as a function of initial SMC; (iii) assess how well within-catchment spatial runoff predictions agreed with 1- to 2-weekly field observations, in particular of overland flow at the microplot scale.

Materials and methods

Study catchment and experimental design

On 27 August 2008, a wildfire consumed almost 68 ha of forest near the village of Colmeal, in the municipality of Góis, north-central Portugal (40°08′42″N, 7°59′16″W; 490 m above sea level (asl)). This burnt area included a small catchment of 10 ha, dominated prior to the fire by maritime pine (*Pinus pinaster* Ait.) stands and eucalypt (*Eucalyptus globulus* Labill.). Land management in this catchment has been extensively described in Vieira *et al.* (2016) and can be summarised as a combination of three forest types (pine and shrubs, eucalypt and shrubs, and eucalypt plantations), and four types of soil mobilisation operations (none, contour ploughing, downslope ploughing and terracing; Fig. 1). As described in Vieira *et al.* (2016, 2018), vegetation and hydrological recovery in the catchment after the 2008 fire were limited as a consequence of past disturbances, especially previous wildfires and the soil mobilisation operations mentioned above.

The climate of the study area can be characterised as humid mesothermal (Köppen Csb, Peel *et al.* 2007), with prolonged dry and warm summers. The mean annual temperature and precipitation at the nearest meteorological station (Góis (station 13I/01G); 10 km) are 12°C and 1133 mm, respectively (SNIRH 2011). The occurrence of precipitation in this area is most frequent between November and February, whereas rainfall events between March and May are less frequent but can have high intensities (Vieira *et al.* 2018).

The parent material in the study catchment consists of pre-Ordovician schists and greywackes (De Brum Ferreira 1978; Pimentel 1994), which have resulted in shallow soils that are typically mapped as Humic Cambisols (Cardoso *et al.* 1971). The A horizons in the study catchment have a coarse sandy loam texture (sand > 70%) and a high stone content (40–46%).

According to field indicators (i.e. canopy and woody and litter consumption, ash colour and mineral soil), the burn severity was low to moderate for vegetation and soil, as tree canopies and logs were only partially consumed, the litter layer was fully consumed, the ash was black and the mineral soil was unaffected (Hungerford 1996; DeBano *et al.* 1998).

After the fire, the catchment was instrumented with a hydraulic channel (H flume) that was equipped with an ultrasonic water level sensor and a rain gauge (0.2 mm tips) connected to a Campbell data logger (CR1000) to measure rainfall and streamflow with 10-min resolution during 4 post-fire years. Additional field measurements of SMC, surface runoff, ground cover and SWR were taken at several points in the burned area. SMC was registered continuously at 3–5 cm soil depth (using Decagon EC-5 soil moisture sensors at three locations, one close to a eucalypt plantation (sm1), another near the pines (sm2), and one located at the outlet (Fig. 1*c*). Surface runoff was assessed in 12 microplots (0.25–0.5 m^2), and monitored with a

weekly frequency depending on rainfall (Vieira *et al.* 2016, 2018). At those same microplots, ground cover was also assessed monthly, whereas soil texture, soil depth and soil roughness were characterised once (Vieira *et al.* 2016, 2018). SWR was measured in the field at monthly intervals in a eucalypt plantation and a pine stand. The SWR monitoring sites were selected immediately downstream from the experimental catchment because of the extensive soil disturbance caused by the measurements, but both sites were comparable with the eucalypt and pine stands within the catchment, including vegetation and soil burnt severity. The monthly SWR data were used to identify the periods when soils were likely to be repellent (Supplementary Material S1). Finally, soil texture, soil depth and soil surface roughness were measured once in all microplots.

Model description and input data

The hydrological processes in the catchment were simulated using the Limburg Soil Erosion Model version 2.01 (De Roo *et al.* 1996). OpenLISEM is a process-based and spatially distributed model that simulates rainfall runoff events using a geographic information system (De Roo *et al.* 1996). The processes incorporated in OpenLISEM are precipitation, interception, surface storage, infiltration and water flux into the soil, surface runoff, and channel flow (De Roo *et al.* 1996). Optionally, erosion processes can also be simulated, which was not performed in the present study because it focused on the hydrological processes in the catchment. In this study, infiltration was simulated with the Green–Ampt one-layer method, while overland flow was routed using the steepest descent flow method.

The rainfall input data for OpenLISEM was obtained by summing the registered tips (of 0.2 mm) of a rain gauge located at the outlet over 10 min intervals and this was used as rainfall intensity (mm h^{-1}). In addition, OpenLISEM input maps with a 5 m spatial resolution were created with respect to: location of the catchment outlet; terrain (digital elevation model (DEM)); land cover characteristics (ground cover (–), leaf area index (m^2 m^{-2}), plant height (m), width of impermeable roads (m)); land surface characteristics (random roughness (cm), Manning's n (–), stone fraction (–)); soil physical characteristics (cohesion of bare soil (kPa), cohesion by roots (kPa), aggregate stability (–), median soil texture (μm), soil depth (mm)); soil hydrological characteristics (saturated hydraulic conductivity (mm h^{-1}), soil water tension at the wetting front (cm), saturated soil moisture content (cm^3 cm^{-3}), initial SMC (cm^3 cm^{-3})). The required input data maps are spatially variable, based on differences in land use and management (Table 1). Cohesion by roots, aggregate stability and plant height were estimated to be zero as a consequence of the wildfire. Cohesion of bare soil was set at 20 kPa, while median soil texture was estimated to be 80 μm. The width of impermeable roads was set to 3 m for all grid cells that included the forest tracks in the catchment (Fig. 1). Initial SMC (θ_i, cm^3 cm^{-3}) varied according to what was recorded by the field soil moisture sensors (sm1, sm2 and outlet). Input maps were the same for each event, except for the calibrated parameters, which varied over time and between events (see Event selection criteria and modelling aproach). The spatial resolution of all maps was 5 m and a fixed model time step of 5 s was used.

The outputs used from OpenLISEM simulations for each event were the time series of the simulated quickflow at the outlet, and the spatially explicit map of the surface runoff generated in the catchment. Following Reitz and Sanford (2019), quickflow was defined as the rapidly varying runoff portion of the discharge hydrograph, with the total

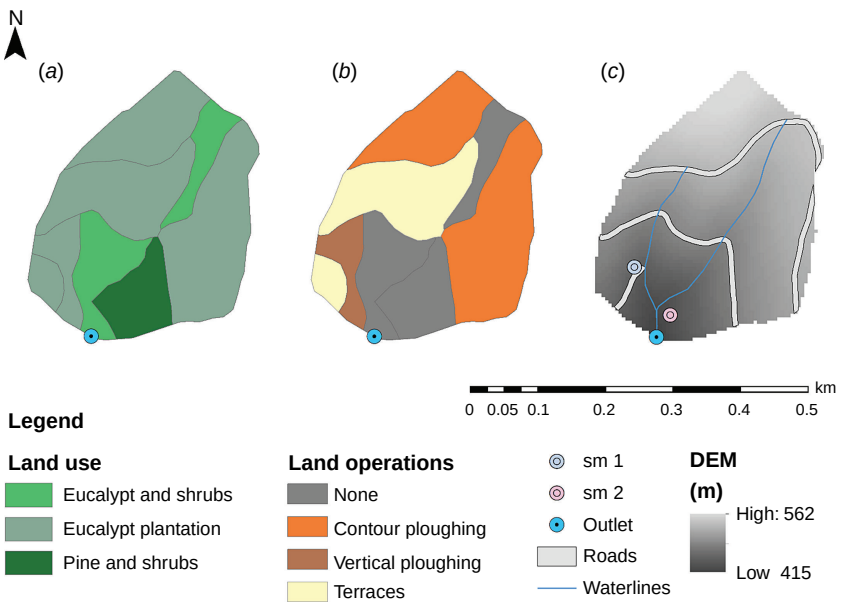

Fig. 1. Colmeal catchment: (*a*) land use; (*b*) land operations; and (*c*) elevation, soil moisture sensor locations (sm 1, sm 2), outlet, roads and waterlines.

Table 1. Model inputs according to land use and land management characteristics.

Land use	Land operations	OpenLISEM inputs									
		Leaf area index (LAI) ($m^2\ m^{-2}$)	Ground cover (–)	Manning's n (–)	Random roughness (cm)	Stone fraction (–)	Sat. hydraulic conductivity ($mm\ h^{-1}$)	Saturated soil moisture content ($cm^3\ cm^{-3}$)	Initial moisture content ($cm^3\ cm^{-3}$)	Soil water tension front (cm)	Soil depth (mm)
Pine and shrubs	None	0.6–1.7	0.69–0.72	**0.06**	2.11	0.12	**30**	**0.44**	sm2	11.01	100
Eucalypt and shrubs	None	1.1–2.3	0.29–0.31	**0.06**	1.84	0.59	**49**		outlet/sm2		250
Eucalypt plantation	Downslope ploughing	1.1–2.0	0.10–0.25	**0.05**	3.91	0.63			sm1		600
Eucalypt plantation	Contour ploughing	1.4–2.5	0.13–0.18	**0.05**	3.79	0.56			sm1		600
Eucalypt plantation	Terraces	1.4–2.5	0.13–0.18	**0.04**	3.68	0.63			sm1		560

Note: bold values were used as base for model calibration according to SWR conditions. Vegetation cover and LAI average values were determined in accordance with the approach of Van Eck *et al.* (2016).

discharge being the sum of quickflow and baseflow. This is illustrated in Fig. 2. Quick flow was derived from the observed streamflow data using the baseflow separation technique proposed by Arnold *et al.* (1995).

Event selection criteria and modelling approach

A total of 16 rainfall runoff events were selected for this modelling exercise (Table 2). All occurred during the first 2 post-fire years, as overland flow generation was most pronounced during this initial phase of the window of disturbance (Vieira *et al.* 2018), and were separated by at least 1 h without rainfall. The 16 events were selected because they had corresponding major quickflow peaks of more than $8\ L\ s^{-1}$, and contrasting initial SMC conditions (Fig. 2). The events were classified into two classes of initial SMC conditions, with 'dry' or 'wet' events having mean SMCs smaller or larger than 17% (Table 2). This threshold value corresponded to the mean SMC conditions over the entire study area. This resulted in seven dry and nine wet events (Table 2). The dry and wet events involved similar median rainfall amounts but with a greater variability in the case of the wet events (Supplementary Fig. S2*d*). The wet events involved consistently higher median and maximum amounts of total quickflow, higher peak quickflows and higher quickflow coefficients than the dry events (Supplementary Fig. S2). Further details on the differences between the wet and dry events are given in Supplementary Material S3.

The modelling procedure included calibration, validation and uncertainty analysis (Fig. 3; see section 2.4). Model calibration, focused on the outlet quickflow, was performed by adjusting three OpenLISEM parameters for each individual event, i.e. Manning's n (n, –), saturated soil moisture content (θ_s, $cm^3\ cm^{-3}$), and saturated hydraulic conductivity (Ksat, $mm\ h^{-1}$) (Table 1). The calibration procedure involved multiplying the respective input maps by a multiplication factor. A similar calibration was applied by Vieira *et al.* (2014) and Nunes *et al.* (2016) for burned areas; however, these prior studies involved seasonal and daily time steps as opposed to the sub-hourly time step used here.

The events were randomly separated into a calibration and a validation dataset, by alternately selecting events from wet and dry datasets (Table 2). An autocalibration was then performed and an optimal parameter set was obtained for the wet and dry calibration events respectively (Fig. 3, Table 2). To assess the feasibility of a calibration validation split test for distinct moisture classes, the optimal parameters were then applied for the validation events (Fig. 3, Table 2), and the resulting model performance was compared with an independent autocalibration for the validation events alone. The split test is frequently used in hydrological modelling studies to provide a test of the statistical significance of the model performance metrics (Liu *et al.* 2018).

Besides the simulation of repellent conditions, other improvements were implemented in the current study

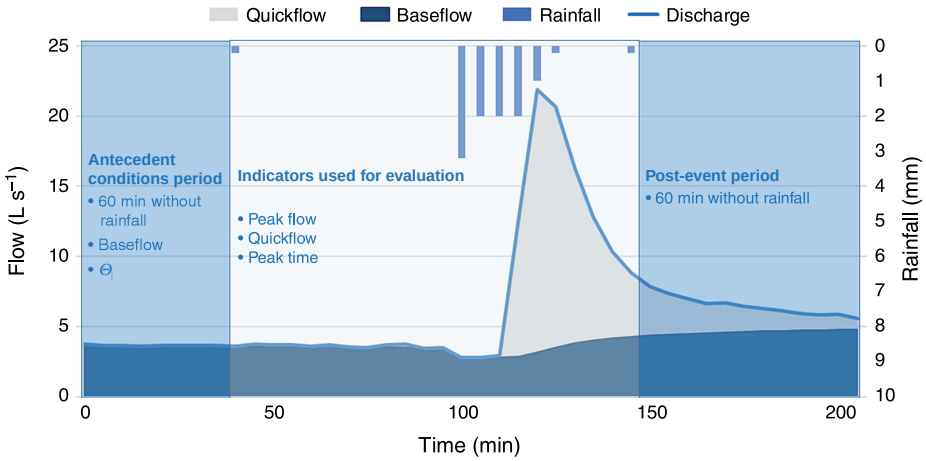

Fig. 2. Schematic representation of hydrological event with a single peak. Discharge flow as light blue line, overlapped by baseflow in dark blue area, and quickflow (discharge minus the baseflow) in grey area. Three panels identify antecedent conditions (left), event (middle), and post-event periods (right), as well as their criteria for event separation and indicators used. The left panel illustrates the time frame in which baseflow and initial soil moisture content (θ_i) were determined.

following the simulations of Van Eck *et al.* (2016), such as the inclusion of forest roads, the resolution increase (10 vs 5 m grid size), which led to the decrease of the simulation time step (5 s), the selection of more events to be simulated (5 vs 16), the inclusion of continuous soil moisture sensor data (Fig. 1) and the uncertainty analysis. Nevertheless, other methodological options taken by Van Eck *et al.* (2016) were kept, such as the land use and the land operations delineation areas as well as most of the physical soil parameter values (Table 1).

In addition to the model calibration and validation focused on quickflow at the outlet, we also validated the spatial maps of runoff generated by OpenLISEM, by comparing them with runoff measurements obtained from microplots within the catchment (0.25–0.5 m^2).

Model performance, fitting and uncertainty analysis

Model performance for quickflow simulations was evaluated for: (i) total quickflow (m^3); (ii) peak flow (L s^{-1}) until a maximum of four peaks per event; and (iii) timing of the peaks (min) until a maximum of four peaks per event. Three commonly used statistical indicators (Moriasi *et al.* 2015) were calculated for each of the three model outputs (i–iii) to assess model performance:

- Nash–Sutcliffe efficiency (NSE) – determines the relative magnitude of the residual variance compared with the measured variance. NSE values larger than 0.5 indicate satisfactory model performance and values > 0.8 indicate very good model performance (Moriasi *et al.* 2015)
- Coefficient of determination (R^2) – describes the proportion of data variance explained by the model. R^2 ranges from 0 to 1, with values higher than 0.5 indicating reasonable model performance (Santhi *et al.* 2001; Van Liew *et al.* 2003).
- Percentage bias (PBIAS) – indicates the magnitude of model errors compared with measurements. Positive PBIAS values indicate model underestimation and negative values model overestimation (Vijai *et al.* 1999). PBIAS values smaller than ±15% for runoff are considered satisfactory (Moriasi *et al.* 2015).

It should be noted that these metrics and thresholds referenced in Moriasi *et al.* (2015) are indicative for daily timesteps, whereas in the current study, model performance was evaluated for hydrographs at the catchment outlet using measured data with 10 min temporal resolution, and by comparing them with the modelled hydrograph.

Autocalibration for the split-test (calibration and validation, Fig. 3, Table 2) was performed executing a constrained fitting of the model to quickflow with *R*. This fit was executed with a model fitting function (modFit), under the Pseudo-random Search Optimisation Algorithm (Price 1977). Parametric uncertainty for each event was obtained by applying a Markov Chain Monte Carlo (MCMC) function in R (modMCMC). Both model fitting and MCMC procedure consisted of 1000 iterations of the chosen parameters under the lower and upper provided bounds, executed under the Flexible Modelling Environment (FME) package in R (Soetaert and Petzoldt 2010), which has been previously applied for hydrological modelling with Soil and Water Assessment Tool (SWAT) (Wu and Liu 2012).

Finally, three statistical models were built to predict Manning's n, Ksat and θ_s: one model for all the events (overall), and two others considering wet and dry conditions separately. This was intended to relate the autocalibration results to several additional explanatory variables in an attempt to understand which variables better explain the obtained model calibration. This was done in Rstudio with the linear model (Chambers and Hastie 1992) function lm {stats}, considering as response variables the calibrated Manning's n, Ksat and θ_s, and as possible explanatory variables the Antecedent Precipitation Index from the 10 days prior to the simulated event (API, –), baseflow at the beginning of the event (L s^{-1}), event rainfall duration (min), maximum rainfall intensity (mm h^{-1}), initial soil moisture content (θ_i, cm^3 cm^{-3}), time since fire (days) and total

Table 2. List and characteristics of all the simulated events.

Class	Event code	Calibration or validation	Date (dd-mm-yy)	Time since fire (days)	Antecedent precipitation (10 days) (mm)	Antecedent precipitation index (API)	Initial moisture conditions ($cm^3\ cm^{-3}$)				Baseflow at the start of the event ($L\ s^{-1}$)	Event rainfall		
							Point		Mean					
							sm1	sm2	Outlet	Catchment		Rain (mm)	Duration (min)	Max Intensity ($mm\ h^{-1}$)
Dry	a	Cal.	17-04-09	232	69.8	32.48	0.11	0.19	0.18	0.13	3.43	20.2	290	16.8
	b	Val.	24-05-09	269	2.2	0.94	0.05	0.08	0.10	0.06	0.52	15.4	160	92.4
	c	Cal.	25-05-09	270	19.0	14.19	0.09	0.17	0.15	0.11	1.42	16.4	250	14.4
	d	Val.	06-06-09	282	11.4	9.12	0.09	0.17	0.12	0.11	1.01	27.6	350	40.8
	e	Cal.	01-12-09	460	61.0	31.00	0.16	0.21	0.21	0.17	5.09	19.6	430	1.2
	f	Val.	20-03-10	569	9.6	6.70	0.16	0.17	0.19	0.17	3.63	17.8	450	19.2
	g	Cal.	15-04-10	595	24.4	18.84	0.15	0.20	0.23	0.16	3.63	10.8	80	38.4
Wet	h	Cal.	22-12-09	481	51.0	25.57	0.17	0.22	0.22	0.18	2.41	33.4	560	18.0
	i	Val.	30-12-09	489	140.0	47.76	0.24	0.24	0.22	0.24	14.00	7.8	70	14.4
	j	Cal.	30-12-09	489	147.6	50.78	0.25	0.25	0.23	0.25	14.59	16	150	26.4
	k	Val.	14-01-10	504	73.0	40.97	0.24	0.26	0.24	0.25	13.35	23	120	28.8
	l	Cal.	25-02-10	546	109.6	48.85	0.21	0.26	0.24	0.22	23.08	20.2	145	38.4
	m	Val.	25-02-10	546	122.0	59.55	0.22	0.27	0.24	0.23	44.89	6.8	60	21.6
	n	Cal.	26-02-10	547	144.8	56.87	0.21	0.20	0.21	0.21	14.67	45.2	500	14.4
	o	Val.	27-02-10	548	166.6	76.80	0.27	0.26	0.25	0.27	42.47	9.8	100	28.8
	p	Cal.	07-03-10	556	111.6	27.96	0.24	0.22	0.22	0.23	7.72	7.0	55	16.8

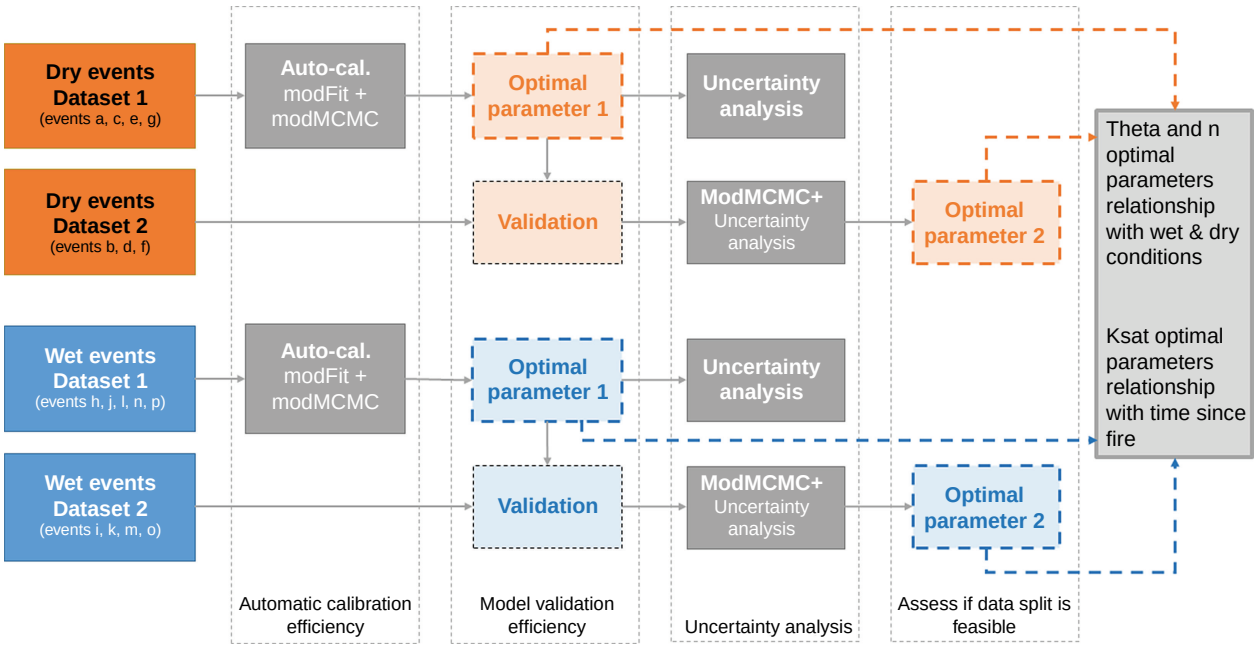

Fig. 3. Modelling approach scheme.

Table 3. OpenLISEM calibration range inputs and model performance for quickflow calibration of individual events.

Class	Event code	Autocalibration + MCMC				
		Manning's n (−)	Ksat (mm h^{-1})	θ (cm^3 cm^{-3})	NSE	R^2
Dry	a	0.28–0.42	35–57	0.25	0.80	0.81
	c	0.39–0.59	5–9	0.29	0.82	0.83
	e	0.36–0.54	11–17	0.33	0.97	0.98
	g	0.38–0.58	14–23	0.27	0.97	0.97
Wet	h	0.40–0.60	45–74	0.34	0.74	0.75
	j	0.24–0.36	12–19	0.34	0.93	0.95
	l	0.34–0.50	59–97	0.31	0.78	0.82
	n	0.39–0.59	5–9	0.41	0.77	0.84
	p	0.31–0.46	7–11	0.41	0.91	0.93

event rainfall (mm). A compilation of these explanatory variables can be found in Supplementary Table S2.

Results

Hydrological response calibration, validation and uncertainty

Autocalibration with OpenLISEM allowed the prediction of the hydrological response of individual events at the catchment outlet with a good to very good model performance (NSE ranging from 0.74 to 0.97; Table 3, Fig. 4). When evaluating OpenLISEM performance for all calibrated events combined (overall), results showed very good model performance in predicting total quickflow, peak flows and time of the peak (Table 4). However, when splitting these events by moisture class (see Supplementary Material S3), OpenLISEM performed better for wet (NSE ranging from 0.83 to 1.00) than for dry conditions (NSE between 0.52 and 1.00), with the latter showing a satisfactory (NSE 0.52) model performance for peak flow, and very good for total quickflow (NSE 0.95) and time of the peak (NSE 1.00).

The validation results were not entirely satisfactory as can be seen by the decrease in model performance, especially for total quickflow and peak flow (Table 4, Fig. 4).

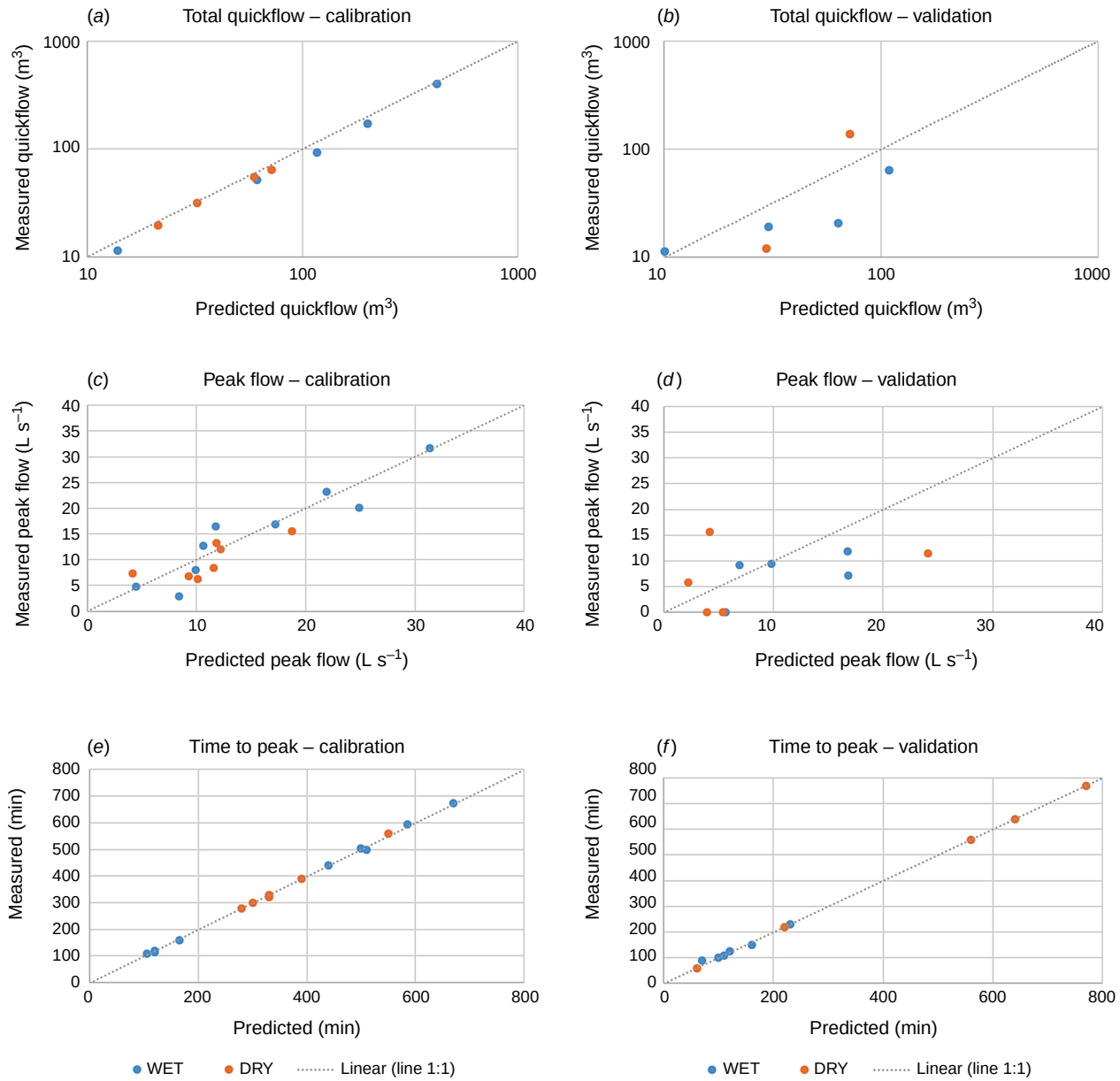

Fig. 4. Measured and OpenLISEM simulated (*a*, *b*) total quickflow ($n = 16$); (*c*, *d*) peak flows ($n = 28$); and (e, *f*) time to peak ($n = 28$) for calibration (*a*, *c*, e) and validation (*b*, *d*, *f*) respectively. Details on modelling approach and data used for calibration and validation can be found in Fig. 3 and Table 2.

Autocalibration results with this specific dataset also showed lower model performances in comparison with the calibration ones (Table 4), especially for total quickflow by obtaining a model performance below the satisfactory level (NSE 0.46) for the overall dataset. Despite that, the resulting decrease in model performance for validation events was still far from the autocalibrated one (Table 4), suggesting that either OpenLISEM is very sensitive for small changes between event characteristics or that the calibrated dataset was not robust enough for a split test.

The linear regression for all optimal parameter sets using the observed auxiliary variables (Supplementary Table S1) showed that wet and dry events were affected by distinct combinations of variables besides initial SMC alone. Still, splitting the data by SMC facilitates the calibration procedure as shown by the increased adjusted R^2 for wet and dry conditions when compared with all events combined (Supplementary Table S1).

The uncertainty analysis performed for each event through the MCMC procedure also showed that a small input variation can result in substantial changes in the quickflow predictions (Supplementary Figs S5, S7, S9, S11). In the illustrated event c (Fig. 5), quickflow prediction varied between 0 and 10 $L\,s^{-1}$ for the first quickflow peak, and 3

Table 4. OpenLISEM model efficiency for calibration and validation datasets.

		Total quickflow (m^3)			Peak flow ($L\,s^{-1}$)			Timing of the peak (min)		
		NSE	R^2	PBIAS (%)	NSE	R^2	PBIAS (%)	NSE	R^2	PBIAS (%)
Calibration (dataset 1)	Overall	0.99	1.00	−9.46	0.80	0.88	−5.49	1.00	1.00	0.18
	Dry	0.95	1.00	−8.11	0.52	0.72	−13.45	1.00	1.00	0.22
	Wet	0.98	1.00	−9.77	0.83	0.96	−1.08	1.00	1.00	0.16
Validation (dataset 2)	Overall	−0.21	0.42	−20.13	−0.12	0.88	10.08	1.00	1.00	0.42
	Dry	−2.22	0.99	24.86	−0.10	0.72	−48.04	1.00	1.00	0.91
	Wet	0.29	0.92	−45.64	−0.19	0.96	61.05	0.97	1.00	−1.27
Calibration (dataset 2)	Overall	0.46	0.88	−36.14	0.89	0.88	−15.02	1.00	1.00	0.00
	Dry	0.11	0.85	−38.38	0.92	0.72	−18.85	1.00	1.00	0.00
	Wet	0.53	0.96	−34.87	0.81	0.96	49.22	1.00	1.00	0.00

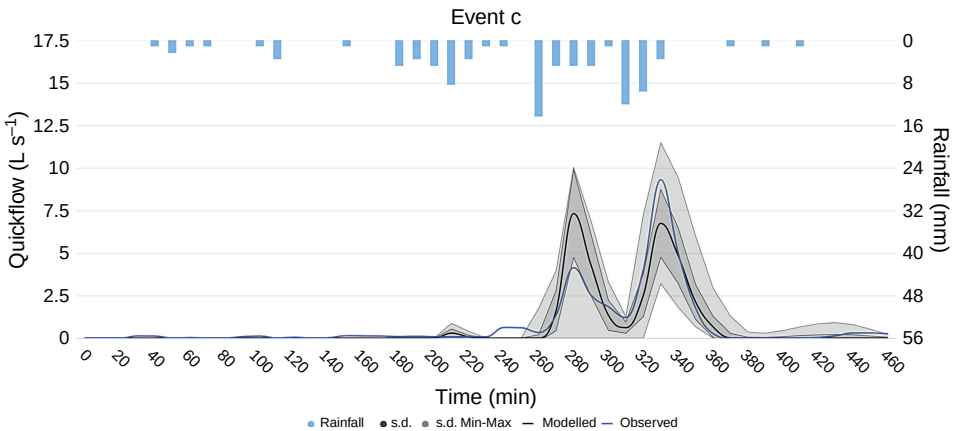

Fig. 5. OpenLISEM quickflow predictions variation for event c simulation following 1000 MCMC iterations with NSE > 0.5. Note minimum and maximum quickflow predictions in light grey range, quickflow predictions standard deviation in dark grey range, best quickflow prediction as black line, and observed quickflow as blue line.

and $12\,L\,s^{-1}$ for the second quickflow peak, with small variations of Manning's n (0.39 – 0.59) and Ksat (5 – $9\,mm\,h^{-1}$). Nevertheless, despite these uncertainties in predicting total quickflow and peak flows, the timing of the peaks was constantly predicted in line with the observed timing of the flow.

Spatial field validation

The most notable result was that very low or sometimes no surface runoff was predicted by OpenLISEM on two slopes where field microplots were installed and runoff was observed (Supplementary Figs S6, S8, S10, S12). Those plots were located at Eucalypt contour ploughed and Eucalypt downslope ploughed sites. On the remaining plots (Pine unploughed site), model simulations presented a better agreement with the field visits during wet events than when compared with the dry events, but in general OpenLISEM simulated lower runoff amounts than those measured by all field plots (Fig. 6). Additionally, the connectivity between the upper part of the catchment and the bottom part near the outlet was only verified in 63% of the simulated events (e.g. events a, b Fig. 7), which is less than was verified with field observations (75%) concerning those specific events, whereas the remaining events presented a contributing area limited to the Pine site and the road adjacent to the outlet (event i, Supplementary Fig. S10).

The validation of the model simulations with the field data at microplot scale revealed limitations due to the different time steps used (event vs weekly). The primary reason for those limitations was the fact that the rainfall event contribution to the total hydrological response of that week was highly variable (17–97%).

Discussion

Approaching hydrological response predictions by considering SWR

In this study, we calibrated OpenLISEM through varying Manning's n, Ksat and θ_s according to an SMC threshold for catchment dryness or wetness at the beginning of each event. This study hypothesised that such classification could potentially be used as a proxy for SWR. However, in the same way as the preceding study (Van Eck *et al.* 2016), the main difficulties found in the simulation of quickflow with

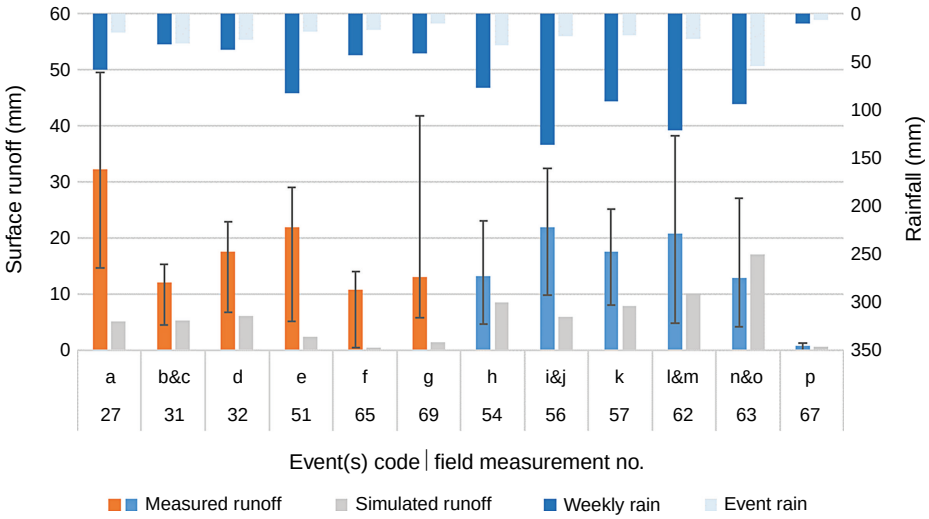

Fig. 6. Rainfall for weekly field monitoring (dark blue, upper axis) vs measured runoff at microplots (orange for dry and blue for wet, bottom axis), and event rainfall (light blue, upper axis) vs simulated event runoff (grey, bottom axis) with the OpenLISEM model at the Pine unploughed site. Note field measurements nos 31, 56, 62 and 63 had more than one event in that week.

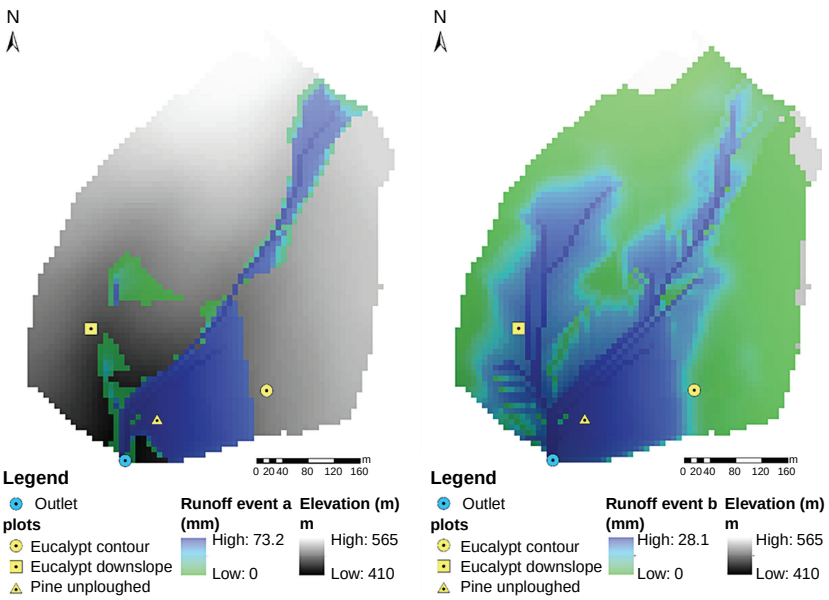

Fig. 7. OpenLISEM spatial runoff predictions for events (*a*) (left), and (*b*) (right) for optimal parameterisation set.

OpenLISEM were associated with the occurrence of SWR and its spatial and temporal expression, as shown by the lower model performance for drier conditions (Table 3).

Our results showed that the current classification for wet or dry conditions may require some improvement, by detailing such classification for each land use or operation, or by considering an SMC gradient along the catchment. There are some approaches for SMC or soil hydrological properties based on topographic analysis that can provide a reasonable estimation to improve hydrological modelling (Nunes *et al.* 2009; Tavares Wahren *et al.* 2016).

To overcome the low resolution of SWR measurements, exploring continuous SMC data as an indicator of SWR was expected to be a promising alternative, primarily because of the well-known relationship between SWR and SMC (Doerr and Thomas 2000; Malvar *et al.* 2016; Robichaud *et al.* 2016), and secondly, because it would be available through the use of sensors, independently of the event timing. However, it seems that other variables besides SMC interfere in the hydrological response at this scale, as demonstrated by the multiple significant relationships between the calibrated inputs and other auxiliary variables such as API, time since fire, baseflow or rainfall characteristics (Supplementary Table S1). For example, the rainfall conditions in the wet events were similar between the calibration and validation events, while dry events showed greater dispersion in the auxiliary variables. This may have been one of the reasons why model performance on validation was not entirely successful. Therefore, we hypothesise that future modelling exercises at these spatial and temporal scales may require a greater number of events for calibration, thus allowing integration of larger hydrological variability.

Despite the limited results, we still consider that OpenLISEM could be improved by including an SWR module,

which would limit the water infiltration capacity in the presence of SWR conditions or the presence of low SMC. This could be done through the reduction of θ_s throughout the entire event, as performed in this study, or only during a short initial stage of the rainfall event, as verified in several field observations, whereas the SWR barrier breaks at a certain rainfall amount or SMC threshold (Crockford *et al.* 1991; Doerr and Thomas 2000; Malvar *et al.* 2016; Mao *et al.* 2019); this approach was successfully tested by Nunes *et al.* (2016) for SWR breaking after a sequence of wet days.

Model performance and comparison with other studies

The calibration results showed good agreement between observed and simulated total flow and peak flow at the outlet. However, PBIAS analysis showed some level of underestimation of the total flow and peak flow but still with good model performance. OpenLISEM had greater difficulties in simulating dry than wet events, whereas peak flows were underestimated for dry conditions, as shown by the satisfactory PBIAS metrics. Similar results were also found by Van Eck *et al.* (2016), where OpenLISEM underestimated flows under prevalent SWR conditions, but overestimated flows when SWR was less prevalent. The validation results, however, showed that the number of events used was not sufficient to provide a robust calibration with OpenLISEM regarding total flow and peak flow. Nonetheless, it seemed sufficient to accurately predict the peak timing, which is an excellent result for predicting extreme events and helps to improve preparedness in facing possible hydrological and erosive risks downstream.

In terms of spatial simulation of runoff, OpenLISEM revealed poor agreement with field measurements, by simulating limited or no runoff in two out of three monitored slopes (Figs 6, 7). This also happened in other studies with this same model (Jetten *et al.* 2003), with this problem being attributed to an inadequate infiltration estimation or problems in the flow network, which was not identified in the current study. This disagreement occurred for two slopes (eucalypt) that had been subjected to land operations (contour and downslope ploughing), and this difference between simulations and reality came from the elevated infiltration simulated in these locations, as a consequence of the higher surface roughness and the greater soil depth. Additionally, OpenLISEM also presented difficulties in addressing catchment connectivity, especially in wet conditions, when baseflow was larger. The fact that OpenLISEM cannot simulate baseflow, even when an accurate SMC at the beginning of the event is provided, may lead to a limited connection between slopes, especially near the streams where soils are likely nearly saturated in wet conditions (Supplementary Fig. S8).

The methodological approach used in this study to address post-fire conditions and SWR through the calibration of events according to their moisture class allowed good overall model performance to be obtained but also revealed several difficulties in adjusting infiltration through θ_s. A similar approach was taken by Moussoulis *et al.* (2015) who assessed the effect of SWR in their runoff predictions by calibrating the threshold depth for infiltration with Système Hydrologique Européen (MIKE SHE) (Abbott 1986) in seven partially burned catchments in Greece. Moussoulis *et al.* (2015) also calibrated Manning's n for the peak flow size and timing, obtaining a satisfactory to good model performance at a monthly scale, whereas at a daily time-step, MIKE SHE was not satisfactory. Without addressing SWR specifically but only addressing post-fire conditions, Seibert *et al.* (2010) suggested the best calibration to address fire-induced changes would be by reducing water storage capacity within the Hydrologiska Byråns Vattenbalansavdelning (HBV) model (Bergstrom 1992), which is in line with the proposed changes in the present study. Alternatively, Canfield *et al.* (2005), Goodrich *et al.* (2005), Rengers *et al.* (2016, 2019) and Wu *et al.* (2021*a*, 2021*b*) suggested that post-fire hydrological calibrations should be focused on Ksat and Manning's n, which would lead to higher runoff peaks without a dramatic increase in runoff volume. The calibration of Canfield *et al.* (2005) resulted in good to very good NSE performances for individual events; however, events resulting in an NSE below 0.7 were removed from their analysis. Wu *et al.* (2021*a*, 2021*b*) obtained satisfactory to very good model performance with automatic calibration for quickflow, whereas Rengers *et al.* (2016, 2019) assessed model performance focusing on peak flow timing for both calibration and validation.

The fairly high post-fire Manning's n estimations obtained after the autocalibration procedure (Table 3) agree with the estimations obtained by Wu *et al.* (2021*a*, 2021*b*) for burned and unburned conditions for the south of Portugal. They can be explained by the deep soil interventions found in these locations such as contour ploughing and terracing (Supplementary Fig. S1), which are frequently found in the Mediterranean landscape (Martins *et al.* 2013), and also supported by the roughness measurements obtained *in situ* (Vieira *et al.* 2016).

For Ksat parameterisation, Ebel and Martin (2017) and Ebel (2020) estimated that Ksat for burned areas should decrease substantially after fire, as a consequence of changes in soil organic matter and soil structure, followed by an increase to background levels during the 4–5 post-fire years. Although the authors could not attribute this recovery to a specific cause, they suggest similarities with mechanisms documented in other studies (e.g. Robichaud *et al.* 2016), where Ksat recovery is driven by vegetation and ground cover recovery. However, during the 2 post-fire years of this study, we only found a significant inverse relationship between Ksat and time since fire (estimate -0.19) for dry events (P-value < 0.001, Adjusted R^2 0.95, Supplementary Table S1). Wu *et al.* (2021*a*, 2021*b*), using the OpenLISEM model in a larger catchment in southern Portugal, did not find a decrease in calibrated Ksat values for post-fire versus pre-fire events.

The application of OpenLISEM to the Colmeal catchment allowed us to accurately predict post-fire hydrological response in a small catchment at the event scale. The approach adopted in this study agrees with the methodologies applied in the limited amount of studies that address post-fire hydrological modelling at catchment scale (Canfield *et al.* 2005; Goodrich *et al.* 2005; Van Eck *et al.* 2016; Rengers *et al.* 2016; Wu *et al.* 2021*a*, 2021*b*), but may still require additional improvement in the classification of SMC and its spatial variability. Nevertheless, our results showed that OpenLISEM can be a promising tool in determining the time of the peak, while less efficiently determining total quickflow and peak flows. Moreover, these predictions were achieved in great detail, whereas most studies addressing this matter use daily to monthly time-steps (e.g. Dun *et al.* 2009; Mahat *et al.* 2015; Seibert *et al.* 2010), and often involve the study of partially burned catchments (e.g. Moussoulis *et al.* 2015; Nunes *et al.* 2018; Basso *et al.* 2020). In this sense, we believe this study can provide new insights about post-fire hydrological modelling by studying the hydrological response from several individual rainfall events in an entirely burned catchment. Although the Colmeal catchment is small (10 ha), the knowledge created in this study could be scaled up to bigger catchments, which have often been highlighted to potentially cause serious off-site effects after a fire (Moody *et al.* 2013; Ebel 2020; Santi and Rengers 2020).

Conclusions

This study aimed to improve the understanding of the hydrological response of recently burnt catchments and, in particular, the role of SWR through the application of the process-based rainfall runoff OpenLISEM model.

After this modelling exercise, we conclude that calibration of OpenLISEM for post-fire hydrological response at catchment scale resulted in accurate simulations at the outlet, especially for quickflow, peak flows and timing of the peaks. Still, the poor validation results for quickflow and peak flows reveal OpenLISEM's high sensitivity to specific event conditions and indicate that the number of calibrated events was not enough to perform a robust calibration.

Model calibration for two distinct initial SMCs showed lower model performance in predicting post-fire hydrological response for dry conditions, which presumably are under higher influence of SWR. Splitting the dataset for wet and dry conditions allowed determination of which other variables influenced model parameterisation besides initial SMC, and also allowed verification that future model calibration can benefit from such splitting.

The validation of the OpenLISEM spatially distributed runoff simulations revealed comparability problems and poor agreement with field surface runoff measurements within the monitored slopes. Additionally, field evidence shows that OpenLISEM failed to properly describe catchment connectivity between ploughed slopes and near streams, likely owing to an overestimation of the infiltration simulated in these slopes, and also because the model does not simulate baseflow.

This modelling exercise revealed that OpenLISEM has strong potential to simulate post-fire hydrological response, especially if an SWR component can be considered in the simulations, and if more detailed information is provided to the model, namely high resolution of SWR measurements and spatially distributed SMC.

Supplementary material

Supplementary material is available online.

References

Abbott MB, Bathurst JC, Cunge JA, O'Connell PE, Rasmussen J (1986) An introduction to the European Hydrological System — Systeme Hydrologique Europeen, 'SHE', 1: History and philosophy of a physically based, distributed modelling system. *Journal of Hydrology* **87**, 45–59. doi:10.1016/0022-1694(86)90114-9

Arnold JG, Allen PM, Muttiah R, Bernhardt G (1995) Automated base flow separation and recession analysis techniques. *Groundwater* **33**, 1010–1018. doi:10.1111/j.1745-6584.1995.tb00046.x

Basso M, Vieira DCS, Ramos TB, Mateus M (2020) Assessing the adequacy of SWAT model to simulate postfire effects on the watershed hydrological regime and water quality. *Land Degradation & Development* **31**, 619–631. doi:10.1002/ldr.3476

Bergström S (1992) The HBV model – its structure and applications. SMHI (Hydrology, Research Department, SMHI). http://urn.kb.se/resolve?urn=urn:nbn:se:smhi:diva-2672

Calheiros T, Pereira MG, Nunes JP (2021) Assessing impacts of future climate change on extreme fire weather and pyro-regions in Iberian Peninsula. *Science of The Total Environment* **754**, 142233. doi:10.1016/j.scitotenv.2020.142233

Canfield HE, Goodrich DC, Burns IS (2005) Selection of parameters values to model post-fire runoff and sediment transport at the watershed scale in southwestern forests. In 'Managing Watersheds for Human and Natural Impacts Engineering. Ecological Economic Challenges'. (Ed Moglen GE) pp. 1–12. (American Society of Civil Engineers). https://doi.org/10.1061/40763(178)48.

Cardoso JC, Bessa MT, Marado MB (1971) Carta dos solos de Portugal - 1:1.000.000. Agr. Lusitana 33 (1–4), 481–602.

Cerdá A, Doerr SH (2005) Influence of vegetation recovery on soil hydrology and erodibility following fire: an 11-year investigation. *International Journal of Wildland Fire* **14**, 423–437. doi:10.1071/WF05044

Chambers JM (1992) Lineal models. In 'Statistical models in S'. (Ed Chambers JM, Hastie TJ). pp. 317–321. (Physica-Verlag HD)

Crockford H, Topalidis S, Richardson DP (1991) Water repellency in a dry sclerophyll eucalypt forest — measurements and processes. *Hydrological Processes* **5**, 405–420. doi:10.1002/hyp.3360050408

DeBano LF (2000) The role of fire and soil heating on water repellency in wildland environments: a review. *Journal of hydrology* **231**, 195–206. doi:10.1016/S0022-1694(00)00194-3

DeBano LF, Neary DG, Ffolliott PF (1998) 'Fire Effects on Ecosystems.' (John Wiley & Sons: New York, NY) Available at https://books.google.com/books?id=cFxtriC2EDkC&pgis=1

De Brum Ferreira A (1978) 'Planaltos e montanhas do Norte da Beira.' (Estudo de Geomorfologia)

Dekker LW, Doerr SH, Oostindie K, Ziogas AK, Ritsema CJ (2001) Water repellency and critical soil water content in a dune sand. *Soil Science Society of America Journal* **65**, 1667–1674. doi:10.2136/sssaj2001.1667

Doerr SH, Thomas AD (2000) The role of soil moisture in controlling water repellency: new evidence from forest soils in Portugal. *Journal*

of Hydrology **231–232**, 134–147. doi:10.1016/S0022-1694(00)00190-6

Doerr SH, Shakesby RA, Walsh RPD (1996) Soil hydrophobicity variations with depth and particle size fraction in burned and unburned *Eucalyptus globulus* and *Pinus pinaster* forest terrain in the Águeda Basin, Portugal. *CATENA* **27**, 25–47. doi:10.1016/0341-8162(96)00007-0

Doerr SH, Shakesby RA, Walsh Rpd (2000) Soil water repellency: its causes, characteristics and hydro-geomorphological significance. *Earth-Science Reviews* **51**, 33–65. doi:10.1016/S0012-8252(00)00011-8

De Roo APJ, Wesseling CG, Ritsema CJ (1996) LISEM: a single-event physically based hydrological and soil erosion model for drainage basins. I: theory, input and output. *Hydrological processes* **10**, 1107–1117. doi:10.1002/(SICI)1099-1085(199608)10:8<1107::AID-HYP415>3.0.CO;2-4

Dun S, Wu JQ, Elliot WJ, Robichaud PR, Flanagan DC, Frankenberger JR, Brown RE, Xu AC (2009) Adapting the Water Erosion Prediction Project (WEPP) model for forest applications. *Journal of Hydrology* **366**, 46–54. doi:10.1016/j.jhydrol.2008.12.019

Ebel BA (2020) Temporal evolution of measured and simulated infiltration following wildfire in the Colorado Front Range, USA: Shifting thresholds of runoff generation and hydrologic hazards. *Journal of Hydrology* **585**, 124765. doi:10.1016/j.jhydrol.2020.124765

Ebel BA, Martin DA (2017) Meta-analysis of field-saturated hydraulic conductivity recovery following wildland fire: Applications for hydrologic model parameterization and resilience assessment. *Hydrological Processes* **31**, 3682–3696. doi:10.1002/hyp.11288

Ferreira AJD, Coelho COA, Walsh RPD, Shakesby RA, Ceballos A, Doerr SH (2000) Hydrological implications of soil water-repellency in *Eucalyptus globulus* forests, north-central Portugal. *Journal of Hydrology* **231–232**, 165–177. doi:10.1016/S0022-1694(00)00192-X

Goodrich DC, Canfield HE, Burns IS, Semmens DJ, Miller SN, Hernandez M, Levick LR, Guertin DP, Kepner WG (2005) Rapid post-fire hydrologic watershed assessment using the AGWA GIS-based hydrologic modeling tool. In 'Managing Watersheds for Human and Natural Impacts Engineering. Ecological Economic Challenges'. (Ed Moglen GE) pp. 1–12. (American Society of Civil Engineers)

Hungerford RD (1996) 'Soils–fire in ecosystem management notes: unit II–I.' (USDA Forest Service, National Advanced Resource Technology Center: Marana, AZ)

Jetten V, Govers G, Hessel R (2003) Erosion models: quality of spatial predictions. *Hydrological Processes* **17**, 887–900. doi:10.1002/hyp.1168

Keizer JJ, Doerr SH, Malvar MC, Prats SA, Ferreira RS V, Oñate MG, Coelho COA, Ferreira AJD (2008) Temporal variation in topsoil water repellency in two recently burnt eucalypt stands in north-central Portugal. *CATENA* **74**, 192–204. doi:10.1016/j.catena.2008.01.004

Liu D, Guo S, Wang Z, Liu P, Yu X, Zhao Q, Zou H (2018) Statistics for sample splitting for the calibration and validation of hydrological models. *Stochastic Environmental Research and Risk Assessment* **32**, 3099–3116. doi:10.1007/s00477-018-1539-8

Liu T, McGuire LA, Wei H, Rengers FK, Gupta H, Ji L, Goodrich DC (2021) The timing and magnitude of changes to Hortonian overland flow at the watershed scale during the post-fire recovery process. *Hydrological Processes* **35**, e14208. doi:10.1002/hyp.14208

Lopes AR, Girona-García A, Corticeiro S, Martins R, Keizer JJ, Vieira DCS (2021) What is wrong with post-fire soil erosion modelling? A meta-analysis on current approaches, research gaps, and future directions. *Earth Surface Processes and Landforms* **46**, 205–219. doi:10.1002/esp.5020

Mahat V, Anderson A, Silins U (2015) Modelling of wildfire impacts on catchment hydrology applied to two case studies. *Hydrological Processes* **29**, 3687–3698. doi:10.1002/hyp.10462

Malvar MC, Prats SA, Nunes JP, Keizer JJ (2016) Soil water repellency severity and its spatio-temporal variation in burnt eucalypt plantations in North-Central Portugal. *Land Degradation & Development* **27**, 1463–1478. doi:10.1002/ldr.2450

Mao J, Nierop KGJ, Dekker SC, Dekker LW, Chen B (2019) Understanding the mechanisms of soil water repellency from nano-scale to ecosystem scale: a review. *Journal of Soils and Sediments* **19**, 171–185. doi:10.1007/s11368-018-2195-9

Martins MAS, Machado AI, Serpa D, Prats SA, Faria SR, Varela MET, González-Pelayo, Keizer JJ (2013) Runoff and inter-rill erosion in a Maritime Pine and a Eucalypt plantation following wildfire and terracing in north-central Portugal *Journal of Hydrology and Hydromechanics* **61**(4), 261–268. doi:10.2478/johh-2013-0033

Martins MAS, Verheijen FGA, Malvar MC, Serpa D, González-Pelayo O, Keizer JJ (2020) Do wildfire and slope aspect affect soil water repellency in eucalypt plantations? – A two-year high resolution temporal dataset. *CATENA* **189**, 104471. doi:10.1016/j.catena.2020.104471

McGuire LA, Rengers FK, Kean JW, Staley DM, Mirus BB (2018) Incorporating spatially heterogeneous infiltration capacity into hydrologic models with applications for simulating post-wildfire debris flow initiation *Hydrological Processes* **32**(9), 1173–1187. doi:10.1002/hyp.11458

Moody JA, Shakesby RA, Robichaud PR, Cannon SH, Martin DA (2013) Current research issues related to post-wildfire runoff and erosion processes. *Earth-Science Reviews* **122**, 10–37. doi:10.1016/j.earscirev.2013.03.004

Moriasi DN, Gitau MW, Pai N, Daggupati P (2015) Hydrologic and water quality models: Performance measures and evaluation criteria. *Transactions of the ASABE* **58**, 1763–1785. doi:10.13031/trans.58.10715

Moussoulis E, Mallinis G, Koutsias N, Zacharias I (2015) Modelling surface runoff to evaluate the effects of wildfires in multiple semi-arid, shrubland-dominated catchments. *Hydrological Processes* **29**, 4427–4441. doi:10.1002/hyp.10509

Nunes JP, Seixas J, Keizer JJ, Ferreira AJD (2009) Sensitivity of runoff and soil erosion to climate change in two Mediterranean watersheds. Part II: Assessing impacts from changes in storm rainfall, soil moisture and vegetation cover. *Hydrological Processes* **23**, 1212–1220. doi:10.1002/hyp.7250

Nunes JP, Malvar M, Benali AA, Rial Rivas ME, Keizer JJ (2016) A simple water balance model adapted for soil water repellency: application on Portuguese burned and unburned eucalypt stands. *Hydrological Processes* **30**, 463–478. doi:10.1002/hyp.10629

Nunes JP, Doerr SH, Sheridan G, Neris J, Santín Nuño C, Emelko MB, Silins U, Robichaud PR, Elliot WJ, Keizer J (2018) Assessing water contamination risk from vegetation fires: Challenges, opportunities and a framework for progress. *Hydrological Processes*. doi:10.1002/hyp.11434

Peel MC, Finlayson BL, McMahon TA (2007) Updated world map of the Köppen–Geiger climate classification. *Hydrology and Earth System Sciences* **11**, 1633–1644. doi:10.5194/hess-11-1633-2007

Pimentel NL (1994) As formas do relevo ea sua origem. In 'Portugal Perfil Geográfico Editorial Estampa, Lisboa'. (Ed Brito RS) Portugal Perfil Geográfico. pp. 29–50. (Editorial Estampa, Lisboa)

Price WL (1977) A controlled random search procedure for global optimisation. *The Computer Journal* **20**, 367–370. doi:10.1093/comjnl/20.4.367

Reitz M, Sanford WE (2019) Estimating quick-flow runoff at the monthly timescale for the conterminous United States. *Journal of Hydrology* **573**, 841–854. doi:10.1016/j.jhydrol.2019.04.010

Rengers FK, McGuire LA, Kean JW, Staley DM, Hobley DEJ (2016) Model simulations of flood and debris flow timing in steep catchments after wildfire. *Water Resources Research* **52**, 6041–6061. doi:10.1002/2015WR018176

Rengers FK, McGuire LA, Kean JW, Staley DM, Youberg AM (2019) Progress in simplifying hydrologic model parameterization for broad applications to post-wildfire flooding and debris-flow hazards. *Earth Surface Processes and Landforms* **44**, 3078–3092. doi:10.1002/esp.4697

Robichaud PR, Wagenbrenner JW, Pierson FB, Spaeth KE, Ashmun LE, Moffet CA (2016) Infiltration and interrill erosion rates after a wildfire in western Montana, USA. *CATENA* **142**, 77–88. doi:10.1016/j.catena.2016.01.027

San-Miguel-Ayanz J, Moreno JM, Camia A (2013) Analysis of large fires in European Mediterranean landscapes: Lessons learned and perspectives. *Forest Ecology and Management* **294**, 11–22. doi:10.1016/j.foreco.2012.10.050

Santhi C, Arnold JG, Williams JR, Dugas WA, Srinivasan R, Hauck LM (2001) Validation of the SWAT model on a large rwer basin with point and non-point sources1. *JAWRA Journal of the American Water Resources Association* **37**, 1169–1188. doi:10.1111/j.1752-1688.2001.tb03630.x

Santi PM, Rengers FK (2020) 'Wildfire and Landscape Change.' (Elsevier) doi:10.1016/B978-0-12-818234-5.00017-1

Santos JM, Verheijen FGA, Tavares Wahren F, Wahren A, Feger K-H, Bernard-Jannin L, Rial-Rivas ME, Keizer JJ, Nunes JP (2016) Soil water repellency dynamics in pine and eucalypt plantations in Portugal – A high-resolution time series. *Land Degradation & Development* **27**, 1334–1343. doi:10.1002/ldr.2251

Seibert J, McDonnell JJ, Woodsmith RD (2010) Effects of wildfire on catchment runoff response: a modelling approach to detect changes in snow-dominated forested catchments. *Hydrology research* **41**, 378–390. doi:10.2166/nh.2010.036

Shakesby RA (2011) Post-wildfire soil erosion in the Mediterranean: Review and future research directions. *Earth-Science Reviews* **105**, 71–100. doi:10.1016/j.earscirev.2011.01.001

Shakesby RA, Doerr SH (2006) Wildfire as a hydrological and geomorphological agent. *Earth-Science Reviews* **74**, 269–307. doi:10.1016/j.earscirev.2005.10.006

SNIRH (Serviço Nacional de Informação sobre Recursos Hídricos) (2011). Available at https://snirh.apambiente.pt/

Soetaert K, Petzoldt T (2010) Inverse modelling, sensitivity and Monte Carlo analysis in R using package FME. *Journal of statistical software* **33**, 1–28.

Stoof CR, Vervoort RW, Iwema J, Elsen E, Ferreira AJD, Ritsema CJ (2012) Hydrological response of a small catchment burned by experimental fire. *Hydrology and Earth System Sciences* **16**, 267–285. doi:10.5194/hess-16-267-2012

Tavares Wahren F, Julich S, Nunes JP, Gonzalez-Pelayo O, Hawtree D, Feger K-H, Keizer JJ (2016) Combining digital soil mapping and hydrological modeling in a data scarce watershed in north-central Portugal. *Geoderma* **264**, 350–362. doi:10.1016/j.geoderma.2015.08.023

Turco M, Llasat M-C, von Hardenberg J, Provenzale A (2014) Climate change impacts on wildfires in a Mediterranean environment. *Climatic Change* **125**, 369–380. doi:10.1007/s10584-014-1183-3

Turco M, Bedia J, Di Liberto F, Fiorucci P, von Hardenberg J, Koutsias N, Llasat M-C, Xystrakis F, Provenzale A (2016) Decreasing fires in Mediterranean Europe. *PLOS ONE* **11**, e0150663. doi:10.1371/journal.pone.0150663

Van Liew MW, Arnold JG, Garbrecht JD (2003) Hydrologic simulation on agricultural watersheds: Choosing between two models. *Transactions of the ASAE* **46**, 1539. doi:10.13031/2013.15643

Viedma O, Moity N, Moreno JM (2015) Changes in landscape fire-hazard during the second half of the 20th century: Agriculture abandonment and the changing role of driving factors. *Agriculture, Ecosystems & Environment* **207**, 126–140. doi:10.1016/j.agee.2015.04.011

Vieira DCS, Malvar MC, Fernández C, Serpa D, Keizer JJ (2016) Annual runoff and erosion in a recently burn Mediterranean forest – The effects of plowing and time-since-fire. *Geomorphology* **270**, 172–183. doi:10.1016/j.geomorph.2016.06.042

Van Eck CM, Nunes JP, Vieira DCS, Keesstra S, Keizer JJ (2016) Physically based modelling of the post-fire runoff response of a forest catchment in central Portugal: Using field versus remote sensing based estimates of vegetation recovery. *Land degradation & development* **27**, 1535–1544. doi:10.1002/ldr.2507

Vieira DCS, Prats SA, Nunes JP, Shakesby RA, Coelho COA, Keizer JJ (2014) Modelling runoff and erosion, and their mitigation, in burned Portuguese forest using the revised Morgan–Morgan–Finney model. *Forest Ecology and Management* **314**, 150–165. doi:10.1016/j.foreco.2013.12.006

Vieira DCS, Malvar MC, Martins MAS, Serpa D, Keizer JJ (2018) Key factors controlling the post-fire hydrological and erosive response at micro-plot scale in a recently burned Mediterranean forest. *Geomorphology* **319**, 161–173. doi:10.1016/j.geomorph.2018.07.014

Vijai GH, Soroosh S, Ogou YP (1999) Status of automatic calibration for hydrologic models: Comparison with multilevel expert calibration. *Journal of Hydrologic Engineering* **4**, 135–143. doi:10.1061/(ASCE)1084-0699(1999)4:2(135)

Wu J, Baartman JEM, Nunes JP (2021*a*) Testing the impacts of wildfire on hydrological and sediment response using the OpenLISEM model. Part 2: Analyzing the effects of storm return period and extreme events. *CATENA* **207**, 105620. doi:10.1016/j.catena.2021.105620

Wu J, Nunes JP, Baartman JEM, Faúndez Urbina CA (2021*b*) Testing the impacts of wildfire on hydrological and sediment response using the OpenLISEM model. Part 1: Calibration and evaluation for a burned Mediterranean forest catchment. *CATENA* **207**, 105658. doi:10.1016/j.catena.2021.105658

Wu Y, Liu S (2012) Automating calibration, sensitivity and uncertainty analysis of complex models using the R package Flexible Modeling Environment (FME): SWAT as an example. *Environmental Modelling & Software* **31**, 99–109. doi:10.1016/j.envsoft.2011.11.013

Data availability. The data that support the findings of this study are available from the corresponding author, Diana Vieira, on reasonable request.

Conflicts of interest. The authors declare no conflicts of interest.

Declaration of funding. M. Basso is funded by FCT – Fundação para a Ciência e a Tecnologia, I.P., through a PhD fellowship (SFRH/BD/146356/2019). J. P. Nunes is funded by FCT through IF-FCT research grant IF/00586/2015, and J. J. Keizer is funded by FCT through IF-FCT research grant IF/01465/2015. This study was carried out in the framework of the COST Action ES1306: Connecting European Connectivity research, by the FCT national projects EROSFIRE II (PTDC/AGR-CFL/70968/2006) and FEMME (PCIF/MPG/0019/2017). Thanks are due for the financial support to CESAM (UIDP/50017/2020+UIDB/50017/2020), to FCT/MCTES through national funds (PIDDAC) and co-funding by the FEDER, within the PT2020 Partnership Agreement and Compete 2020.

Acknowledgements. We also wish to acknowledge the constructive and valuable comments provided by the editors and reviewers, which remarkably contributed to the improvement of the original manuscript.

Author affiliations

[A]European Commission, Joint Research Centre (JRC), Ispra, Italy.

[B]Centre for Environmental and Marine Studies (CESAM), Department of Environment and Planning, University of Aveiro, Aveiro 3810-193, Portugal.

[C]Soil Physics and Land Management Group, Wageningen University and Research, The Netherlands.

[D]Centre for Ecology, Evolution and Environmental Changes (CE3C), Faculdade de Ciências, Universidade de Lisboa, 1749-016 Lisboa, Portugal.